EXPERIMENTAL STUDY OF CO_2/O_2 CORROSION ON PIPE-LINES DURING CARBON CAPTURE, UTILIZATION, AND STORAGE PROCESS

by

Jintao WENG[a], Xiaoyi ZHOU[b], Tianyu WANG[a*], Meicheng WANG[b], Yawen TAN[a], and Shouceng TIAN[a]

[a] State Key Laboratory of Petroleum Resources and Prospecting, China University of Petroleum, Beijing, China
[b] Fengcheng Oil Plant of Xinjiang Oilfield, Karamay, China

Original scientific paper
https://doi.org/10.2298/TSCI240226185W

In this paper, high temperature and high pressure corrosion test was used to simulate the corrosion process of multi-component thermal fluid ($CO_2/O_2/H_2O$) on oil pipes (N80 steel), casings (J55, TP90H, P110 steel, and transportation pipe-lines (20# steel) in the process of CCUS technology application. The results show that during the entire corrosion process, the oil layer casing and surface casing are corroded most seriously in this environment, and the corrosion forms of these five steel materials in the CO_2/O_2 environment are uniform corrosion and local corrosion, and the corrosion products mainly consist of $FeCO_3$, Fe_2O_3, Fe_3O_4, and FeOOH crystals. These oxides form a double-layer film structure on the surface of the steel. The inner layer is denser and consists mostly of $FeCO_3$ crystals, which has better protection against further corrosion of the internal steel. The outer layer is loose and porous, and its components are mostly $FeCO_3$ crystals. Fe_2O_3, FeOOH, Fe_3O_4, and $FeCO_3$ crystals, have poor corrosion protection for internal steel. Due to the difference in corrosion products of the inner and outer film layers, relatively obvious local corrosion appeared on the surfaces of the five steel materials.

Key words*: CCUS, pipe-lines corrosion, CO_2/O_2 coexistence system, multi-component thermal fluid*

Introduction

The CCUS technology can efficiently achieve deep CO_2 emission reductions [1]. In the CCUS technology chain, transporting captured CO_2 to oil and gas fields for enhanced recovery (CO_2-EOR), but the captured CO_2 fluid usually contains some impurity gases (such as O_2, H_2O*, etc.*) [2]. When these impurities enter all aspects of CO_2 transportation and CO_2-EOR together with compressed CO_2, they will greatly increase the risk of corrosion of pipe strings and downhole tools. Many scholars have conducted corresponding research on the corrosion mechanism of CO_2/O_2 fluid on pipe strings during the application of CCUS technology [3, 4]. In the CO_2 phase with lower H_2O content, steel will hardly corrode. However, as the H_2O content increases, obvious corrosion will occur on the steel. Among them, the corrosion form of CO_2 on the pipe string is mostly uniform corrosion, and the corrosion products are mainly $FeCO_3$ [5] the $FeCO_3$ corrosion product film is dense and has good protection. Sun's research

* Corresponding author, e-mail: wangty@cup.edu.cn

[6] shows that when there is a trace amount of O_2 in the CO_2 environment, the generated Fe_2O_3 corrosion products will destroy the continuity of the $FeCO_3$ film and reduce its protective effect. Dou *et al.* [7] also discovered a similar mechanism, and they also found that the oxides formed by the reaction between O_2 and Fe would cover the surface of $FeCO_3$ irregularly, destroying the structure of the $FeCO_3$ film. Therefore, this article uses high temperature and high pressure corrosion tests to study the corrosion behavior of oil pipes (N80 steel), casings (TP90H steel, P110 steel and J55 steel), and ground gathering and transportation pipe-lines (20# steel) in the CO_2/O_2 environment during the application of CCUS technology. The surface morphology, product composition and corrosion product film characteristics of the corrosion products were analyzed through SEM, EDS, and XRD technology.

Experiments

The experiment used a total of five kinds of steel samples, respectively, N80 steel, TP90H steel, P110 steel, J55 steel and 20# steel, the samples used in the experiment were taken from oil well pipe strings and ground gathering pipe-line strings at an oil field site, these five kinds of steel materials were processed into 50 mm × 10 mm × 3 mm specimens with a hole (D = 4 mm) on one end. The solution used in the experiment simulated the formation water produced on-site in an oil field. The solution composition is shown in tab. 1, the gas medium in this experiment was mainly composed of N_2, CO_2, and O_2 (wherein, N_2:CO_2:O_2 = 73:10:4).

Table 1. Solution ion concentration table of oilfield produced fluids

HCO_3 [mg/L]	CL [mg/L]	Ca^{2+} [mg/L]	Na^+ [ma/L]	Salinitiy [mg/L]	Water type
368.1	2822.4	22.8	1975.1	5296.7	$NaHCO_3$

Table 2. Experimental plan design

Num.	Steel	Oxygen content [%]	Temperature [°C]	Pressure [MPa]
#1	N80	4%	240	8
#2	J55	4%	240	8
#3	TP90H	4%	240	8
#4	P110	4%	240	8
#5	20#	4%	240	8

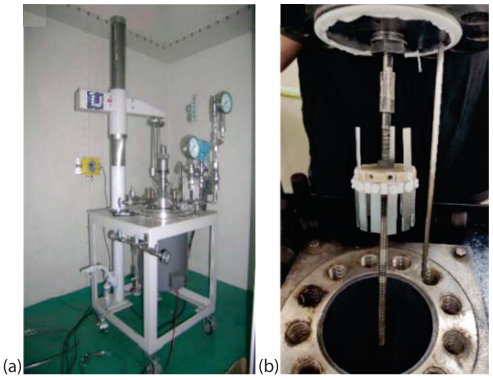

Figure 1. Experimental devices and corrosion pendant installation diagram

This paper uses a high temperature and high pressure corrosion device, shown in fig. 1(a), to simulate the corrosion behavior of five types of steels in a CO_2 transport or injection environment. The test plan is shown in tab. 2, and the experimental steps are:

– The samples are polished and dehydrated, and then weighed and photographed for recording.

– Load the sample on the polytetrafluoroethylene bracket, as shown in fig. 1(b), then inject 1.5 L degassing solution into the autoclave, seal the autoclave, and inject N_2 for degassing.

– Raise the temperature of the system to 240 °C, then fill the reactor with CO_2, O_2, and N_2 in sequence, and conduct a 72 hours corrosion experiment.
– Taking out the corrosion sample from the kettle, take pictures and record them, then dehydrate, dry and pickle them. Finally, weigh and take pictures of the pickled samples.

After the experiment, the steel corrosion rate is calculated, where the steel corrosion rate, r_{corr}, is calculated:

$$r_{corr} = \frac{8.76 \cdot 10^4 (m_o - m_t)}{St\rho} \tag{1}$$

where r_{corr} is the corrosion rate, m_o – the mass of the sample before the experiment, m_t – the mass of the sample after the experiment, S – the total area of the sample tested, ρ – the density of the sample material, and t – the experimental time.

Results

Corrosion rate

Table 3 represents the corrosion rate of N80 steel, TP90H steel, P110 steel, J55 steel, and 20# steel after 72 hours corrosion experiment in high temperature and high pressure reactor. During the entire corrosion process, the corrosion rates of J55 and TP90H casing are the highest, which are 9.54 mm annually and 7.56 mm annually, respectively, followed by N80 oil pipe and P110 casing, whose corrosion rates are 6.70 mm annually and 4.19 mm annually, respectively, 20# steel ground pipe-line has the smallest corrosion rate, its corrosion rate is 2.45 mm annually. According to the GB/T 23258-2020 standard, the corrosion degree of the five types of steel is severe corrosion, and the oil layer casing and surface casing are the most severely corroded in this environment, it can be seen that the pipe string will be severely corroded during the CO_2 transportation or injection process.

Table 3. Corrosion rate chart of 5 types of steel in CO_2/O_2 system

Steel	TP90H	N80	J55	P110	20#
Corrosion rate [mm per year]	7.56	6.70	9.54	4.19	2.45

Corrosion appearance

In the CO_2/O_2 environment, the five types of steel materials experienced obvious uniform corrosion as a whole, and localized corrosion occurred at the lower end of the sample, the macroscopic morphology of the corroded surface is shown in fig. 2. There are many corrosion products formed on the surface of J55 steel, TP90H steel, P110 steel, and N80 steel, the overall color is dark brown and reddish brown. The reddish brown products are mainly iron oxides formed by the oxidation of Fe^{2+} to Fe^{3+}, these corrosion products are loose and porous and easy to fall off, poor protection of internal metal. The corrosion products on the surface of 20# steel are relatively small and distributed in spots, its surface corrosion is relatively uniform and the degree of corrosion is low.

Comparing the matrix morphology of these five samples before and after pickling, it can be found that before pickling, the surfaces of J55 steel, TP90H steel, P110 steel, and N80 steel all have more irregular local convex accumulation phenomena, while after pickling, they can be found that there are obvious corrosion pits at the bottom of these four steel samples. Moreover, the thickness of the base wall at the bottom of these four types of steel is much thinner. The J55 steel and TP90H steel are thinned most significantly, the thickness of the bottom

wall of the two is reduced by 40% and 35%, respectively, and after pickling, the 20# steel are also had small pits evenly distributed on the surface. This shows that these five steel materials have obvious local corrosion phenomena in the CO_2/O_2 coexistence system.

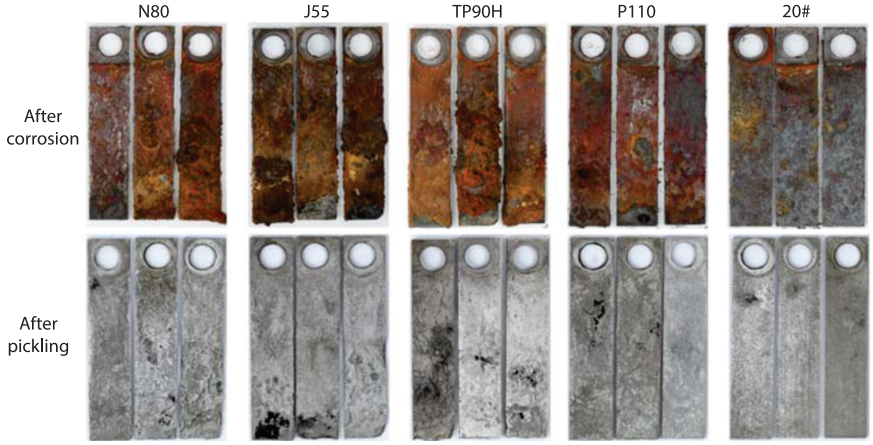

Figure 2. Macroscopic morphology of corroded surfaces of steels before and after pickling

Through macroscopic observation, it was also found that the corrosion product films on the surfaces of these five steels have a double-layer structure. The outer film is loose and easy to fall off, and has poor corrosion protection for the internal steel, while the inner film is relatively dense, which has better protection against further corrosion of internal steel.

Corrosion product film characteristics

Figure 3(a) shows the SEM scanning results of five kinds of steel surface corrosion products, it can be found that the double-layer film structure of these five kinds of steel surface corrosion products is that the outer film is loose and has many holes, and the inner film is denser but has many tiny cracks, there are a large number of nodular protrusions on the inner surface of the product film. Through SEM scanning, it is found that N80 steel, 20# steel, and P110 steel have obvious pinhole-like local corrosion on the surface, while in addition local corrosion, there are also local fractures on the surface of TP90H steel and J55 steel, and the surfaces of these five steel substrates are chaotically distributed.

Combined with EDS scanning, fig. 3(b), it was found that the corrosion products of these five types of steels are mainly composed of C, O, Si, Mn, Fe, and other elements. Among them, the Fe and O contents in the local convex areas of the steel sample are higher than those in the flat areas. Combined with XRD scanning, fig. 3(c), it was found that the components of the granular or needle-shaped corrosion products in the outermost layer of the corrosion products are mostly Fe_2O_3, $F3O_4$, $FeCO_3$, and FeOOH crystals, this layer has poor protection for the metal inside the steel. The product components of the dense film in the inner layer of corrosion products are mostly $FeCO_3$ crystals, which is relatively dense and has better protection for the metal inside the steel. Since a large number of F_3O_4, Fe_2O_3, and FeOOH crystals are generated on the surface of the substrate, these crystals have smaller adhesion on the surface of the substrate than $FeCO_3$ crystals., and are easy to fall off, weakening the the protective effect of the product film on the matrix. Obvious local corrosion appeared on the surface of the five steel materials, and the degree of corrosion was relatively serious. This is also consistent with the results obtained from the macroscopic appearance observation of the corrosion products.

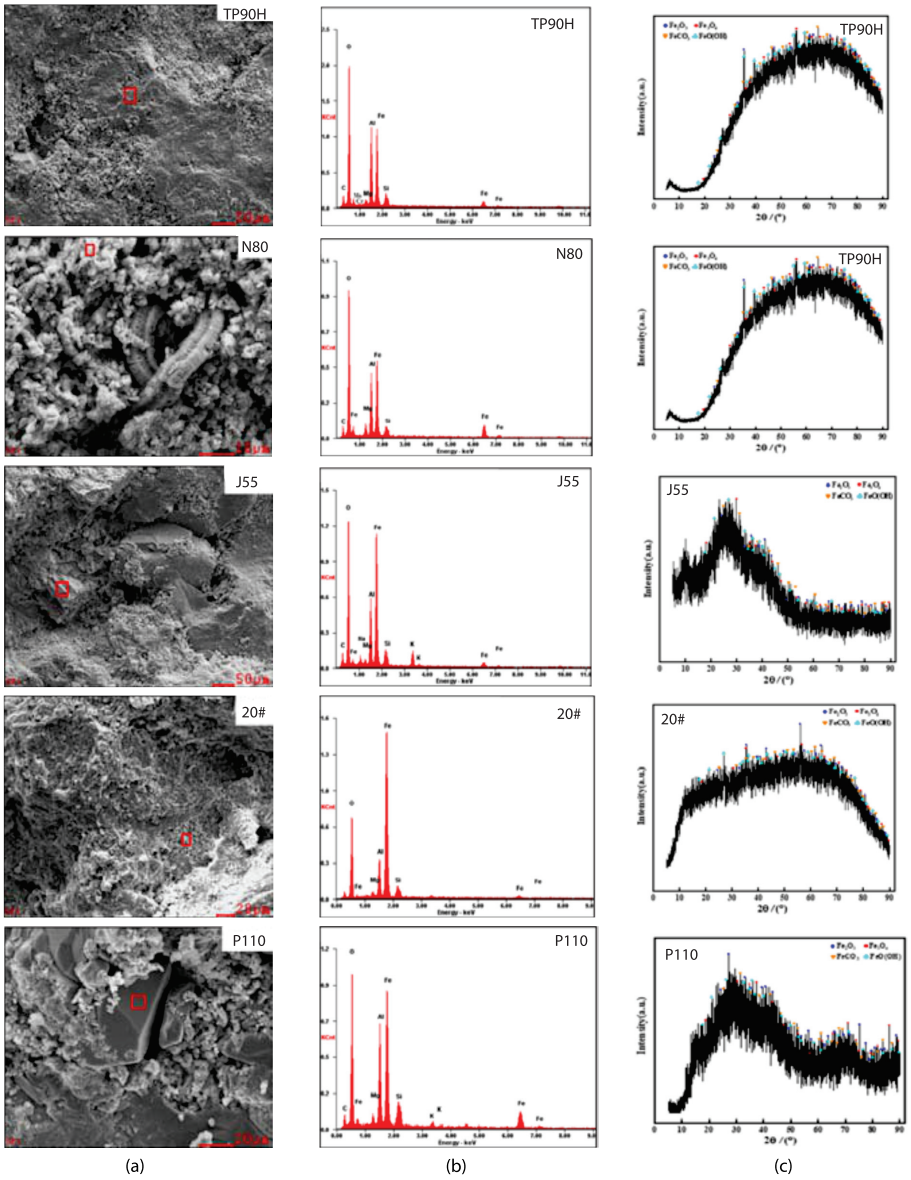

Figure 3. Energy spectrum and XRD patterns of corrosion products of five types of steels; (a) microscopic morphology scan of corrosion products, (b) energy spectrum of corrosion products, and (c) XRD pattern of corrosion products

Conclusion

In CO_2/O_2 environment, J55 and TP90H casing have the highest corrosion rates, followed by N80 oil pipe and P110 casing, and 20# steel ground pipe-line has the smallest corrosion rate. The degree of corrosion of the five types of steel is severe corrosion. The corrosion forms of TP90H steel, N80 steel, J55 steel, 20# steel, and P110 steel in CO_2/O_2 environment are uniform corrosion and local corrosion. Combining the EDS and XRD scanning results, we dis-

cover that the corrosion products generated by these five steel materials are mainly composed of Fe_2O_3, FeOOH, Fe_3O_4, and $FeCO_3$ crystals. The corrosion products generated by the five types of steel have a double-layer film structure. The inner film is relatively dense and contains mostly $FeCO_3$ crystals, which has good protection against further corrosion of the internal steel; while the outer film is loose and porous, mostly composed of Fe_2O_3, FeOOH, Fe_3O_4, and $FeCO_3$ crystals, and has poor corrosion protection for the internal steel.

References

[1] Gimeno, B., *et al*., Influence of SO_2 on CO_2 Transport by Pipe-line for Carbon Capture and Storage Technology: Evaluation of CO_2/SO_2 Cocapture, *Energy and Fuels*, *32* (2018), 8, pp. 8641-8657
[2] Norhasyima, R. S., *et al*., Advances in CO_2 Utilization Technology: A Patent Landscape Review, *Journal of CO_2 Utilization*, *26* (2018), 2, pp. 323-335
[3] Sun, C., *et al*., Probing the Initial Corrosion Behavior of X65 Steel in CCUS-EOR Environments with Impure Supercritical CO_2 Fluids, *Corrosion Science*, *189* (2021), 109585
[4] Yuan, J., *et al*., Corrosion Behavior of Cr-Bearing Steels in CO_2-O_2-H_2O Multi-Thermal-Fluid Environment, *Materials Research Express*, *7* (2020), 10, 106518
[5] Javidi, M., *et al.*, Failure Analysis of a Wet Gas Pipe-Line Due to Localised CO_2 Corrosion, *Engineering Failure Analysis*, *89* (2018), 2, pp. 46-56
[6] Sun, J., *et al*., Effect of O_2 and H_2S Impurities on the Corrosion Behavior of X65 Steel in Water-Saturated Supercritical CO_2 System, *Corrosion Science*, *107* (2016), 3, pp. 31-40
[7] Dou, Y., *et al*., Experimental Study on Corrosion Performance of Oil Tubing Steel in HPHT Flowing Media Containing O_2 and CO_2, *Materials*, *13* (2020), 22, 5214

Paper submitted: February 26, 2024
Paper revised: March 25, 2024
Paper accepted: May 6, 2024